PHYSICAL REVIEW LETTERS

Thermal Diffusion Shock Waves

Sorasak Danworaphong,[1] Walter Craig,[3] Vitalyi Gusev,[4] and Gerald J. Diebold[2]

[1]*Department of Physics, Brown University, Providence, RI 02912, USA*
[2]*Department Chemistry, Brown University, Providence, RI 02912, USA*
[3]*Department of Mathematics, McMaster University, Hamilton, Ontario, Canada L8S 4K1*
[4]*Université du Maine, av. Messiaen, 72085 LeMans, Cedex 09 France*
(Received 15 October 2004; published 10 March 2005)

The Ludwig-Soret effect or thermal diffusion, which refers to the separation of liquid mixtures in a temperature gradient, is governed by a nonlinear, partial differential equation in space and time. It is shown here that the solution to the nonlinear differential equation for a binary mixture predicts the existence of shock waves completely analogous to fluid shocks and obeys an expression for the shock velocity that is an exact analogue of the Rankine-Hugoniot relations. Direct measurements of the time dependent, spatial absorption profile of a suspension of nanometer sized particles subjected to a sinusoidal temperature field generated by a pair of continuous laser beams, as well as self-diffraction experiments, show motion of the particles in agreement with the predictions of nonlinear theory.

Since Ludwig's first observation [1] that Na^+ and Cl^- ions migrate and are concentrated by imposition of a thermal gradient imposed on a salt solution, the separation of the components of a mixture in a thermal field, known as "thermal diffusion," has been found not only in liquids, but also in gases, and even in solids [2–4]. The phenomenon of thermal diffusion, also known as the Soret or Ludwig-Soret effect [5], typically produces a small separation of solvent mixtures; however, when suspensions of nanometer sized particles or solvent mixtures near a consolute critical point are exposed to thermal gradients [4,6] the parameters describing the Ludwig-Soret effect can be large, implying substantial separation of the components. Here we show, for a sinusoidal temperature field in a binary mixture where the Ludwig-Soret effect is large, that moving fronts, or "shock waves," between the components of the mixture are predicted by solution to the nonlinear partial differential equation that describes thermal diffusion. The shock waves that are predicted by the mathematics have properties identical to the familiar shock waves in fluids and obey a mathematical relation for their velocities exactly analogous to the well known Rankine-Hugoniot relations that govern the state variables in a fluid shock. Experiments using crossed laser beams to produce a sinusoidal temperature field in a cell containing nanometer sized iron oxide particles in solution are reported showing multiple diffraction of a laser beam, boundaries in the absorption profiles of the particles characteristic of moving shocks, and a particle distribution in space characteristic of the nonlinearity in the solution to the differential equation describing the Ludwig-Soret effect.

Although a number of methods have been employed over the years for imposing a thermal gradient on a solution to generate thermal diffusion, recently, a new technique based on the interference of two crossed laser beams to form an optical grating in a weakly absorbing fluid has been introduced [4,7–9] that has sizeable thermal gradients, sinusoidal in space, but with only a small overall temperature rise [10]. For a steady temperature field of the form $T = T_0[1 + \sin(Kx)]$, where T_0 is a temperature and K is a wave number determined by the optical fringe spacing in the grating, the Ludwig-Soret effect is governed by [11]

$$\frac{\partial c(z,t)}{\partial \tau} = \alpha \frac{\partial}{\partial z}\{c(z,t)[1 - c(z,t)]\cos z\} + \frac{\partial^2 c(z,t)}{\partial z^2}, \quad (1)$$

where c is the density fraction [12] of the first species, i.e., the mass per unit volume of the first species normalized to the overall mass per unit volume of the solution, $1 - c$ is the density fraction of the second species, α known as the thermal diffusion factor is given by $\alpha = D'T_0/D$, where D is the mass diffusion constant and D' is the thermal diffusion coefficient, and where a dimensionless time τ and coordinate z given by $\tau = K^2Dt$ and $z = Kx$ have been used, where t is the time and x is the coordinate along the grating. It can be seen that Eq. (1) is a partial differential equation in space and time, nonlinear in the density fraction. As in the case of fluid shocks, determination of the important characteristics of the time development of the density fraction is approached by ignoring dissipative effects, in this case, the second term on the right-hand side of Eq. (1) that describes ordinary mass diffusion, which acts to negate the effects of thermal diffusion. Without mass diffusion, the differential equation governing the buildup of c can be written

$$\frac{\partial c}{\partial \tau} = -\frac{\partial f}{\partial z}, \quad (2)$$

where a "flux" $f(c,z)$ is defined as $f(c,z) = -\alpha c(1-c) \times \cos z$. Equation (2) is the differential form of a conservation equation that expresses the buildup of c in a volume as a consequence of a flux change in space. Since for a periodic temperature field the density fraction must be periodic in z, it follows that $c(2\pi, \tau) = c(0, \tau)$; hence, from Eq. (2) the

integral of the density fraction over one optical fringe is independent of time and the law $\int_0^{2\pi} c(z,t)dz = 2\pi c_0$ must be valid for any time t, where c_0 is the density fraction at time $t = 0$, assumed to be a constant throughout the cell. The integral for the density fraction over z expresses simple mass conservation for the Ludwig-Soret effect.

The Eulerian description of the profile $c = c(z, \tau)$ by Eq. (1) can be transformed [13] into a Lagrangian description yielding the coupled pair of ordinary differential equations,

$$\frac{dz}{d\tau} = \frac{\partial f(c, z)}{\partial c} = \alpha(2c - 1)\cos z \qquad (3)$$

$$\frac{dc}{d\tau} = -\frac{\partial f(c, z)}{\partial z} = -\alpha c(1 - c)\sin z, \qquad (4)$$

that gives the motion of points with coordinates $z = z(\tau, c_0 z_0)$ and $c = c(\tau, c_0 z_0)$ on the zc plane for a point initially at $(c_0 z_0)$ at time $\tau = 0$. It is noteworthy that Eqs. (3) and (4) form a Hamiltonian system, analogous to the well known canonical equations of Hamilton found in classical mechanics, with the flux function in the present problem taking on the role of the Hamiltonian function. The motion of any point in the zc plane can be found by eliminating $d\tau$ from Eqs. (3) and (4), which, when integrated [14], yields a constant of the motion k_1

$$c_0(1 - c_0)\cos z_0 = c(1 - c)\cos z = k_1, \qquad (5)$$

from which the locus of points (z, c) in time for a point initially at (z_0, c_0) can be found. A family of trajectories for several values of k_1 is shown in Fig. 1. Equations (5) and (4) can be combined and integrated over a path of constant k_1 to give an exact, albeit implicit, solution for the density fraction versus time as
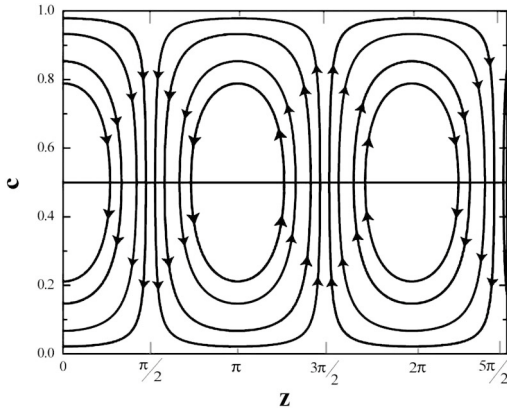

FIG. 1. Portrait of the trajectories of points in the zc plane from Eq. (5) for several values of k_1. Points to the right of $z = 3\pi/2$ with $c < 1/2$ move to the left and upwards initially. As time progresses the points move upwards and to the right giving multiple values for c for a single value of z.

$$F\left[\arcsin\left(\frac{c - 1/2}{b}\right), \left(\frac{b}{a}\right)^2\right] = a(\pm\alpha\tau + k_2), \qquad (6)$$

where F is an elliptic integral of the first kind, the parameters a and b are given by $a = \sqrt{\frac{1}{4} + |k_1|}$ and $b = \sqrt{\frac{1}{4} - |k_1|}$, and k_2 is a constant depending on the initial point of the trajectory [15]. The minus sign is used for points moving in the hot region of the grating $0 < z < \pi$, and the plus sign is used for motion in the cold region $\pi < z < 2\pi$.

A plot of the concentration versus coordinate for several values of the time is given in Fig. 2, which shows that for short times the density fraction of the first species builds up forming progressively higher peaks in the cold region of the grating region (near $z = 3\pi/2$) and decreases in the warm regions. As time progresses, however, the curves take on multiple values of c for a single value of z, at which time the formal solution from the Hamiltonian system is disregarded and the problem is treated by considering the density fraction to behave as a moving discontinuity, or shock wave. The velocity of the right-going shock can be found directly from Eq. (4) as $dz_{sh}/d\tau = [f(c_l, z) - f(c_r, z)]/(c_l - c_r)$, which can be expressed as

$$\frac{dz_{sh}}{d\tau} = \alpha[(c_r + c_l) - 1]\cos z, \qquad (7)$$

where c_l and c_r are the density fractions to the left and to the right of the discontinuity. The shock velocity varies in time and can be seen to slow until it stops when $c_r = 1$ and $c_l = 0$, , i.e., where there is complete separation of the
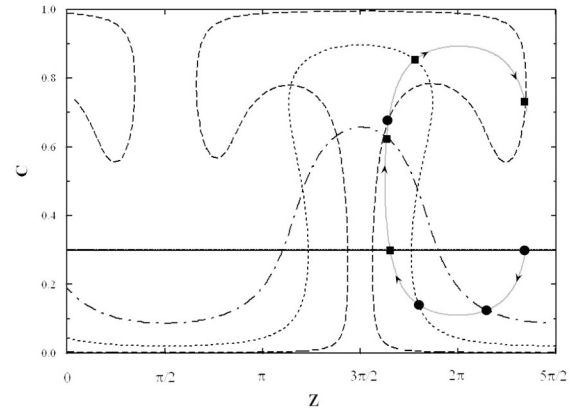

FIG. 2. Density fraction versus dimensionless distance along the grating z for several values of the time from numerical integration of Eqs. (3) and (4) with $\alpha = 15$. The initial density fraction is $c_0 = 0.3$ giving the flat curve; the curves with successively larger values of c at $z = 3\pi/2$ are for values of τ equal to 0, 0.1, 0.2, and 0.4. Since α can be combined with τ in Eq. (1) by division by α to give a time parameter $\alpha\tau$, the curves are universal for values of $\alpha\tau$ equal to 0, 1.5, 3.5, and 6.0. The circles and squares mark the trajectories for two different starting points on the z axis. For positive α, $c(z, \tau)$ builds up in the region near $z = 3\pi/2$; for negative values of α, $c(z, \tau)$ builds up in the region near $z = \pi/2$.

components of the mixture. It is noteworthy that Eq. (7) is an exact analog of the Rankine-Hugoniot relations for one-dimensional fluid shocks: Eq. (7) expresses the thermal diffusion shock velocity in terms of the density fractions on either side of the shock, while the Rankine-Hugoniot relations express the ratios of the state variables of the fluid on either side of the shock in terms of the shock velocity.

Since the effects of diffusion are large when the space gradient of the density fraction is large, numerical integration of Eq. (1) was carried out to determine the influence of mass diffusion on the motion of the shock. It was found that the mass diffusion term produced a smoothing of the features of the shock, but that the motion of a front was still evident, the speed and the sharpness of the front being the highest for large values of α.

It is possible to determine the final distribution of the two species in space with the effects of diffusion included directly from Eq. (1) in closed form by noting that $dc/dt = 0$ at long times. Straightforward integration of Eq. (1) to give the final distribution of $c_N(z) = c(z, \infty)$ when thermal diffusion is exactly balanced by mass diffusion as $c_N(z) = [1 + \bar{F}(\alpha, c_0)e^{\alpha \sin z}]^{-1}$, where $\bar{F}(\alpha, c_0)$ is determined [16] for a given value of α and c_0 through use of the mass conservation law given above. Note that if Eq. (1) is linearized by setting the factor $(1 - c)$ to unity [13] then the corresponding expression for the density fraction $c_L(z)$ is easily found to be $c_L(z) = [c_0/\hat{I}_0(\alpha)] \exp(-\alpha \sin z)$, where $\hat{I}_0$ is a modified Bessel function.

A self-diffraction experiment [17] was carried out by passing the 532 nm beam from a frequency doubled, continuous Nd : YVO$_4$ laser through a Galilean telescope and dielectric beam splitter and recombining the resulting two laser beams in a 10 μm path length Pyrex cell to form a temperature grating, as shown in Fig. 3. The beams were focused to a spot roughly 2 mm in diameter at the front face of the cell; the optical fringe spacing [10] of the grating

was 30 μm. The cell was filled with a suspension of 3 nm Fe$_3$O$_4$ particles in dioctyl adipate with a solution density of 1.2 g/cm^3, which absorbed approximately 80% of the incident 532 nm beam.

The diffracted light pattern from the suspension was recorded photographically on a white card placed approximately 1 m from the cell. As shown in Fig. 4, the two spots from the undiffracted 532 nm beams seen immediately after the laser was switched on were followed by the appearance of a series of equally spaced diffracted light spots [18], with the outermost spots appearing latest in time and with the lowest intensity. The time dependences of the intensities of the diffracted beams, recorded with a photomultiplier and digitizing oscilloscope were fit to a Fourier series decomposition of the density fraction profile determined from numerical integration of Eq. (1) (with diffusion included), giving a fitted value of α equal to -3.6 and a mean value for the rate of change in the width of the density fraction peak of 0.03 μm/s. When one of the laser beams forming the grating was blocked so that only a single beam illuminated the cell, the series of spots from the diffracted beams disappeared over the course of a few minutes, with the outermost spots disappearing most rapidly, eventually leaving only a single spot from the remaining laser beam, the rate of the disappearance being consistent with the highest rate of mass diffusion taking place from the highest spatial harmonics of the density fraction distribution [19].
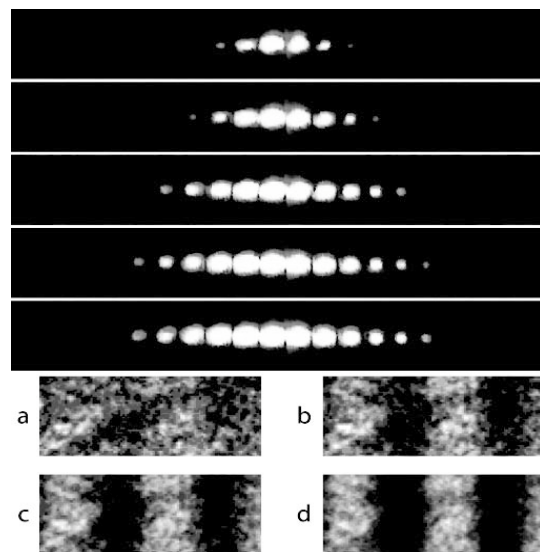
FIG. 4. Top: diffracted light pattern from the laser irradiated cell at five different times showing multiple order diffraction. Since the grating was an absorption grating, the intensity of each diffracted beam can be attributed to a distinct spatial harmonic of the absorption profile. Bottom: CCD camera microphotographs taken at (a) 0 s, (b) 1.8 s, (c) 3.0 s, and (d) 12 s after the laser beam is turned on. The distance between the dark and light regions is 30 μm.
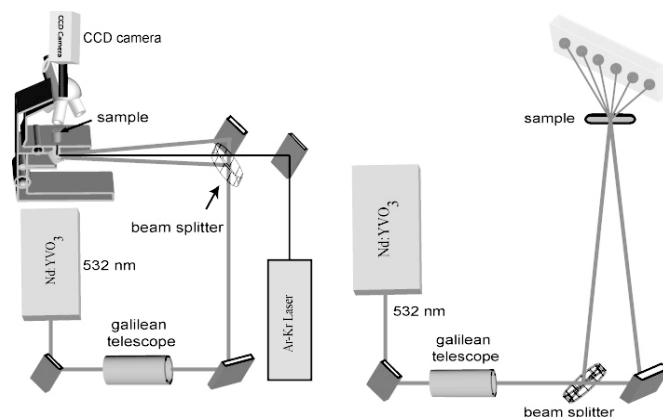
FIG. 3. Diagram of the experimental apparatus for (right) self-diffraction measurements and (left) recording the absorption profile in the cell with a CCD camera. The continuous 532 nm laser was operated to give a power of approximately 200 mW at the front surface of the cell.

Experiments were also carried out using a microscope equipped with a charge coupled device (CCD) camera to view the time development of the absorption profile in the cell directly. A 488 nm beam from a continuous Ar-Kr mixed gas laser provided the illumination for the microscope, which was equipped with narrowband filters to reject the 532 nm beam but pass the 488 nm beam. The absorption in the cell was recorded at periodic intervals after the laser beams were turned on, giving a series of images of the density profile in time. The value of α found from fitting the data to a numerical integration of the absorption profile was -2.7. The absorption profile [20] recorded at long times was fit to both c_N and c_L using the least squares procedure. The latter gave a poor fit to the data, giving a value of the error in the least squares procedure over 3 times that from a fit using c_N, indicating a significant contribution from the nonlinearity in Eq. (1) to the particle distribution.

The origin of thermal diffusion shocks is exactly parallel to that for fluid shocks: both arise from a nonlinearity of the dependent variables in differential equations of motion for the state variables. For thermal diffusion, the density fraction, which constitutes the "state variable," appears with a quadratic dependence in its equation of motion, Eq. (1); for fluid shocks, the pressure, temperature, density, and fluid velocity are the state variables, with the velocity appearing with a quadratic dependence in the conservation equations for both energy and momentum. Of course, a thermal diffusion shock is distinct in its character from a fluid shock as it does not arise from classical Rankine-Hugoniot hydrodynamics. An important difference in the two kinds of shocks is that thermal diffusion depends on the existence of an externally imposed temperature gradient—there is no similar requirement for fluid shocks. A further difference in the two shock phenomena is that in the laboratory observation of the two kinds of shocks, the dissipative force, ordinary mass diffusion in the thermal diffusion shock, as opposed to viscous damping in a fluid shock, is far more dominant in determining the overall spatial profile of the thermal diffusion shock wave. However strongly mass diffusion acts to broaden the features of a thermal diffusion shock, the nonlinearity of Eq. (1) dictates that the motion of the density fraction wave is governed by the mathematics of a shock, and the underlying motion of the components of the mixture is described as a shock phenomenon; the degree to which the shock fronts become easily observable in the laboratory depends solely on the thermal diffusion factor α, the magnitude of which governs the dominance of thermal diffusion over mass diffusion.

[1] C. Ludwig, Sitzber. Akad. Wiss. Vien Math.-naturw. **20**, 539 (1856).
[2] E. A. Mason, R. J. Munn, and R. J. Smigh, in *Advances in Atomic and Molecular Physics*, edited by D. R. Bates (Academic, New York, 1966), p. 33.
[3] R. D. Present, *Kinetic Theory of Gases* (McGraw-Hill, New York, 1958).
[4] W. Köhler and S. Wiegand, in *Thermal Nonequilibrium Phenomena in Fluid Mixtures*, edited by W. Köhler and S. Wiegand (Springer-Verlag, Berlin, 2001), p. 190.
[5] C. Soret, Arch. Sci. Phys. Nat. Geneve **3**, 48 (1879).
[6] M. Giglio and A. Vendramini, Phys. Rev. Lett. **34**, 561 (1975).
[7] K. Thyagarajan and P. Lallemand, Opt. Commun. **26**, 54 (1978).
[8] F. Bloisi, Opt. Commun. **68**, 87 (1988).
[9] W. Köhler, J. Chem. Phys. **98**, 660 (1993).
[10] H. J. Eichler, P. Gunter, and K. W. Pohl, *Laser-Induced Dynamic Gratings* (Springer, New York, 1985).
[11] S. R. deGroot and P. Mazur, *Non-Equilibrium Thermodynamics* (North Holland, Amsterdam, 1962), as noted in this reference the Dufour effect is generally small and can be ignored.
[12] Note that with the negative value of α, for Fe_2O_3 particles in kerosene, means that the particles migrate to the hot regions of the grating, increasing further the temperature gradient so that it is not purely sinusoidal. Experiments where dyes were added to the solution to mitigate this heating effect showed no discernible differences in the density fraction absorption profiles; theoretical simulation of this effect also showed no qualitative change in the behavior of the time development of the density fraction profile.
[13] W. Craig, S. Danworaphong, and G. J. Diebold, Phys. Rev. Lett. **92**, 125901 (2004).
[14] V. Gusev, W. Craig, S. Danworaphong, and G. J. Diebold (to be published).
[15] For points that cross from the cold to the hot region, k_2 must be evaluated for the trajectories in both regions.
[16] $\bar{F}(\alpha, c_0)$ can be written as $(1 - c_\epsilon)/c_\epsilon$ where $c_\epsilon = c(0, \infty)$.
[17] I. Turek, J. Stelina, C. Musil, M. Timko, P. Kopansky, M. Koneracka, and L. Tomco, J. Magn. Magn. Mater. **201**, 167 (1999).
[18] E. Hugonnot, A. Popescu, S. Hanifi-Kadi, and J. P. Delville, Phys. Rev. E **69**, 051606 (2004), time dependent, multiple order diffraction is reported in a photodeposition experiment.
[19] P. Kopcansky, L. Tomco, M. Timko, V. Ocelik, M. Koneracka, I. Turek, J. Stelina, and C. Musil, Acta Physica Polonica A **97**, 875 (2000).
[20] J. C. Bacri, A. Cebers, A. Bourdon, G. Demouchy, B. M. Heegaard, and R. Perzynski, Phys. Rev. Lett. **74**, 5032 (1995), their absorption profile shown in Fig. 1(a) strongly resembles data obtained in the experiments described here.